J. Adhesion Sci. Technol. Vol. 3, No. 4, pp. 261–275 (1989)

Techniques for screening adhesives for structural applications

C. O. ARAH,[1,*] D. K. McNAMARA,[1] H. M. HAND[1] and M. F. MECKLENBURG[2]

[1] *Martin Marietta Laboratories, 1450 South Rolling Road, Baltimore, MD 21227, USA*
[2] *Conservation Analytical Laboratory, The Smithsonian Institution, Washington, DC 20560, USA*

Revised version received 5 December 1988

Abstract—Due to its chemistry, no structural adhesive system (epoxies, acrylics, etc.) is likely to offer an ideal combination of toughness, strength, moisture resistance, and ambient-temperature curing. Therefore, for effective use of adhesives in primary structures, an engineer must be able to identify adhesives that represent an optimum compromise among the different properties.

In this paper, we present techniques for screening high-strength, ambient-temperature-curing adhesives for (1) moisture resistance under sustained loading and (2) fracture resistance in a way that is directly related to joint performance.

Keywords: Screening structural adhesives; stress relaxation; fracture toughness; structural joints; ambient-temperature-curing adhesives.

1. INTRODUCTION

The long-term stability of any adhesively bonded joint is limited by the response of the adhesive to environmental factors, primarily moisture. The strength of an adhesive joint deteriorates rapidly when it is exposed to the high end of temperatures and relative humidities within the usual service environment of the structure. Furthermore, the rate of such environmental attack is accelerated under sustained (creep) loading.

This lack of durability in adverse environments has limited the use of adhesives in primary load-bearing structures. If such joints are to become feasible and reliable over the long-term, three primary problems must be solved: (1) the low tensile and peel strengths of ambient-temperature-curing adhesives, which must be compensated for by oversized, i.e. heavier, joint designs; (2) the inadequate environmental durability, i.e. resistance to moisture and temperature, of the adhesives; and (3) the low fracture toughness of the adhesives, which is so poorly understood that prediction of design safety margins is impossible. So far, advances in adhesive formulations that have ameliorated one of these problems have generally adversely affected the others.

The proposed use of adhesive bonding for metal–composite joints, such as for the Army's lightweight bridge applications, will thus require the development of new, strong, moisture-resistant, ambient-temperature-curing structural adhesives. Working under an Army program, we formulated several such promising

*To whom correspondence should be addressed.

adhesives but, in testing them, found that we had to evaluate both their moisture resistance and fracture toughness, since ductility (as measured by neat film flexing) consistently decreased with increasing moisture resistance. Specifically, we needed a cost-effective technique for screening over 100 different adhesive specimens for moisture sensitivity under sustained loading and for resistance to crack growth in a way that is directly related to joint performance.

2. EXPERIMENTAL PROCEDURES

2.1. Test methods

2.1.1. Moisture resistance. We first attempted to evaluate the moisture resistance of our adhesives by testing tensile strips of adhesives that had been equilibrated in a $>80\%$ relative humidity (RH) and 49°C (120°F) environment; however, we rarely found significant changes in ultimate tensile strengths and elongations under these conditions, i.e. moisture alone did not drastically affect the properties of most of the adhesives [1]. Rather, it is the combination of stress and moisture that actually causes joint failure. Therefore, we selected the stress-relaxation test to evaluate our formulations, since this test measures the strain sustained by adhesives exposed to a moist, warm environment while under stress.

2.1.2. Fracture toughness. Our purpose in testing our modified adhesives for fracture resistance was to characterize this property reliably so that it could be related to joint performance (e.g. enable modifications to adhesive chemistry to be correlated with adhesive fracture parameters). A review of fracture characterization options indicated that the most useful parameters for our purposes would be the elastic energy released, the plastic energy dissipated, and the potential energy of the test specimen at any crack extension. Linear elastic fracture mechanics (LEFM), which is widely used to characterize these materials, would not be applicable as ductility or plastic deformation increased. Similarly, we rejected the use of the J integral, a single-value parameter that combines both elastic and plastic energy components of crack-growth resistance, as a fracture criterion. We needed a clearer distinction of these energies because some types of polymer modification could affect only one energy component. The J integral is, however, useful for comparative purposes.

The method we chose for characterization was an energy separation technique [2], which clearly distinguishes crack growth energies and employs a standard, single-specimen, unload compliance test procedure commonly used in J-integral testing [3].

2.2. Sample preparation and testing

2.2.1. Moisture resistance. To cast adhesive specimens for stress relaxation/tensile measurement, we poured the thoroughly mixed adhesive composition onto an aluminum block $12 \times 5 \times 1$ in. ($30.5 \times 12.7 \times 2.5$ cm) covered with a silicone release sheet, placed another sheet on top, and rolled the adhesive pool with a rolling pin to remove entrapped air. An aluminum block with four 10-mil (0.025 cm) shims glued to its corners was then placed on top of the sheet, and the entire assembly was clamped. The adhesive was allowed to cure for 7 days at

ambient temperatures, or for 2 days at 50°C. All the adhesives mentioned in this paper were post-cured at 50°C for 2 days.

A strip of adhesive, 4–5 in. long, 0.20 in. wide, and 0.010 in. thick (10.2–12.7 × 0.5 × 0.025 cm), was placed under roughly 10% of its ultimate strain in a self-contained stress jig (Fig. 1) positioned inside a humidity chamber [4]. The relaxation of the stress as the adhesive stretched caused a logarithmic decrease in the stress level until it reached a new equilibrium after several hours. At that point, another increment of strain was applied. The result is a measure of the sustainable stress as a function of the strain for an adhesive in equilibrium with its environment. Three strips of each adhesive were tested.

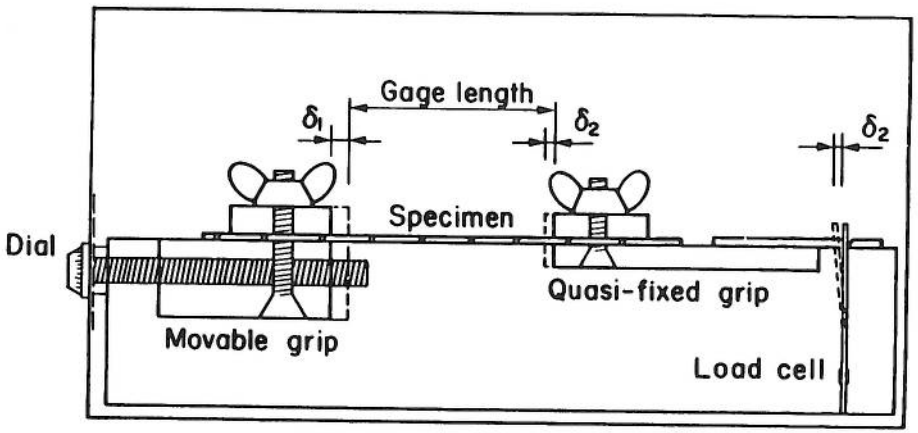

Figure 1. Device for tensile and stress-relaxation measurements.

2.2.2. Fracture toughness. Specimens for toughness testing were 1/2T compact tension plan neat adhesive or bonded, with specimen width $B = 0.25$ in. (0.6 cm). Neat specimens were side-grooved to give a net specimen width between side grooves $B_n = 0.20$ in. (0.5 cm), while bonded specimens were ungrooved, i.e. $B_n = 0.25$ in. (0.6 cm). The dimensions of the specimens are shown in Fig. 2. The clip gage load-line attachment points were made integral to the specimen.

The bulk specimens were cast in aluminum molds coated with release agents. Adherends for the bonded specimens were machined from aluminum (6061-T6) and bonded in alignment jigs to provide a bondline thickness of about 10–25 mils (0.025–0.067 mm). Initial starter cracks were made with razor blades to a crack length of approximately 0.509 in. (1.3 cm). During testing, we determined the crack length, a, using the unload slope and the empirical equations provided in ASTM E1152 [3, 5]. In general, we have found that the crack length can be obtained more accurately if the unloading is at least 20% of the current maximum load. Measured crack lengths agreed well with those calculated by the empirical equation for both the neat and the bonded compact tension specimens. The results of this comparison are presented in Fig. 3.

The elastic modulus, E, was determined in a tensile test on neat specimens as the slope of the elastic region of the stress/strain diagram, and was used for both the crack length determination and the calculation of K_q. For the bonded specimens, we used the modulus of the aluminum.

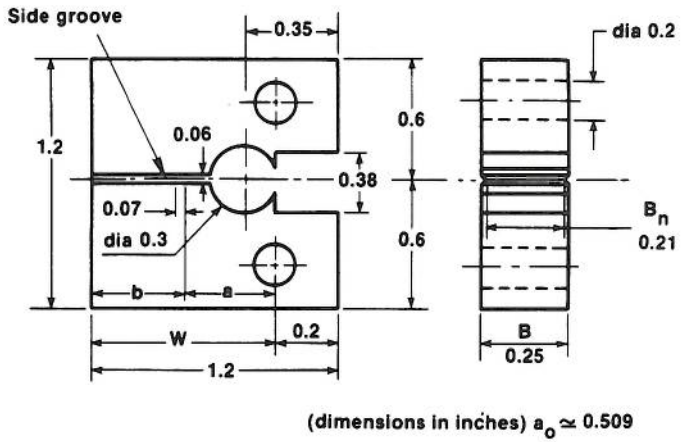

Figure 2. Dimensional diagram of 1/2T plan compact tension specimen.

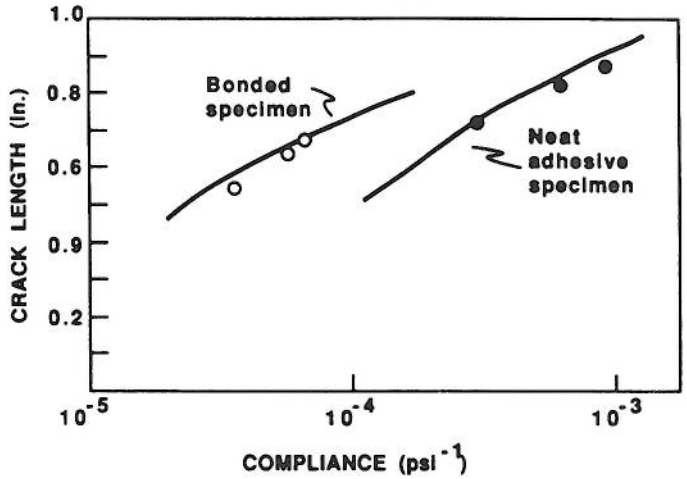

Figure 3. Comparison of the calculated (solid line) and the experimental (circles) crack lengths as a function of the compliance.

3. COMPUTATION METHODS

3.1. Equilibrium stress–strain

Cured adhesives contain little moisture. When subjected to environmental stress, they absorb moisture from the ambient environment until they are in equilibrium with it. Imposition of an additional stress causes further moisture absorption until a new equilibrium is established. Conversely, they lose water when the stress is reduced.

The environmental strains of thermal expansion and moisture swelling on an adhesive specimen are therefore additive with mechanical strains, and both must be considered in determining the strength limits of the adhesive. The environmental strains alone can exceed the elastic limit strain of an adhesive with poor temperature and moisture resistance.

The equilibrium stress–strain curves for our test adhesives 100 and 96 are

shown in Fig. 4. The strain was incremented in predetermined steps and the specimens were tested until failure in an environmentally controlled chamber (Fig. 1) [4]. During this time, the adhesive stress-relaxed under quasi-fixed displacements. The locus of the lowest points of all stress-relaxation segments represents the equilibrium tensile stress–strain curve, i.e. where the moisture content in the adhesive is in equilibrium with the RH of the environment. The size of the strain increment has no effect on the equilibrium stress–strain curve in the linear elastic region [4].

Three mechanisms appear to cause the bulk adhesive specimen to stress-relax above and beyond normal viscoelastic relaxation [4]. The first is water absorption from the surrounding environment. A state of strain changes the volume of a unit cubic element by

$$\delta V = (1 + \varepsilon_x)(1 + \varepsilon_y)(1 + \varepsilon_z) - 1, \tag{1}$$

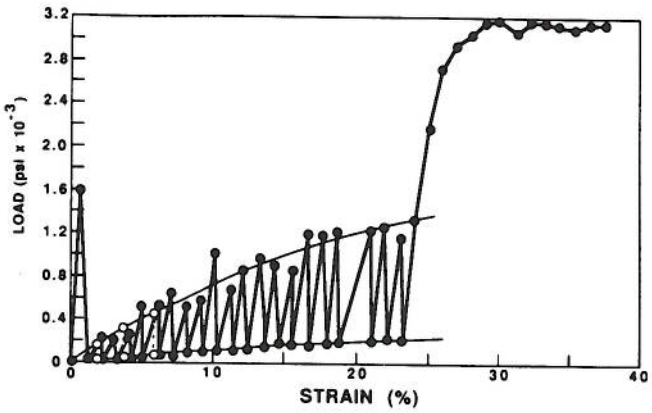

(a)

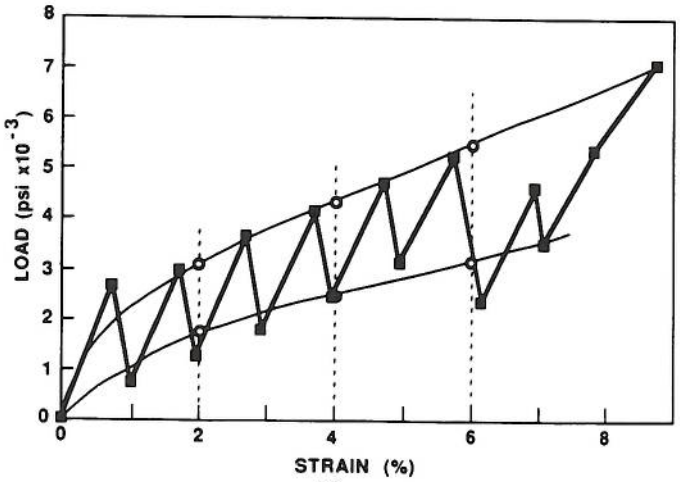

(b)

Figure 4. Stress-relaxation records of adhesives 100 (a) and 96 (b).

or, for small deformations,

$$\delta V = \varepsilon_x + \varepsilon_y + \varepsilon_z. \tag{2}$$

A longitudinal strain increment $\Delta\varepsilon_x$ produces lateral concentrations, $\Delta\varepsilon_y = \Delta\varepsilon_z = -\nu\Delta\varepsilon_x$. Substituting these values and $\Delta\varepsilon_x = \Delta\sigma_x/E$ into equation (2) gives

$$\delta V = \Delta\sigma_x(1 - 2\nu)/E, \tag{3}$$

where δV is the unit change in volume, or volumetric strain, $\Delta\sigma_x$ is the stress increment, E is the rapid-loading modulus, and ν is Poisson's ratio.

The increase in adhesive volume described by equation (3) also increases its water capacity, so that it absorbs additional water from the environment until it is again in equilibrium with the RH of the environment. As the additional moisture swells the adhesive, the stress relaxes under fixed displacement.

The second mechanism of stress relaxation is the reorganization of water molecules lodged between the polymer chains. The pressure exerted by lateral adhesive contraction induced by Poisson's effect could force the water molecules to rotate and displace into positions that would allow additional lateral contraction and, hence, stress relaxation under fixed displacement.

The third mechanism involves the breakage of crosslinks, which allows the polymer chains to slide past each other until new links form.

The dominant mechanisms in the linear elastic region of the stress–strain diagram appear to be water absorption and internal reorganization. Breakage of crosslinks becomes pronounced as the 'yield' point of the adhesives is approached. The first two mechanisms are reversible while the third is not. Currently, there is no method of separating the contributions of each mechanism to the total stress relaxation.

3.2. Fracture analysis: the energy separation method

The area under the plot of a load versus load-line displacement record is the sum of all of the energies—elastic, plastic, and potential—applied to a fracture test specimen during crack initiation and extension. The work, W, done by the external load, P, can be related to the internal energy, U, by

$$\mathrm{d}W = \mathrm{d}U_s + \mathrm{d}U_e + \mathrm{d}U_p, \tag{4}$$

where W is the work done by the external load, U_s is the stored elastic (potential) energy, U_e is the elastic energy released during crack extension, and U_p is the plastic energy dissipated during crack extension.

These energies are depicted in Fig. 5, which illustrates an unload compliance, load versus load-line displacement record for a neat adhesive 1/2T compact tension plan specimen. Here, the specimen is side-grooved 20%, i.e. $B = 0.25$ in. (0.6 cm) and $B_n = 0.20$ in. (0.5 cm). In this figure,

Area OAA′O′ $= U_p$
Area O′A′B $= U_e$
Area O′BD $= U_s$ after crack extension (U_{si+1})
Area OAC $= U_s$ prior to crack extension (U_{si}).

The total resistance to a crack-growth increment, da, is the sum of the plastic

energy dissipated, dU_p, and the elastic energy released, dU_e. The total rate of energy release and dissipation during crack growth can be expressed mathematically as

$$J_{es} = G_{es} + I = 1/B_n dU_e/da + 1/B_n dU_p/da, \quad (5)$$

where J_{es} is the total energy release rate, G_{es} is the elastic energy release rate, I is the plastic energy dissipation rate, B_n is the net specimen width between side grooves, and a is the crack length.

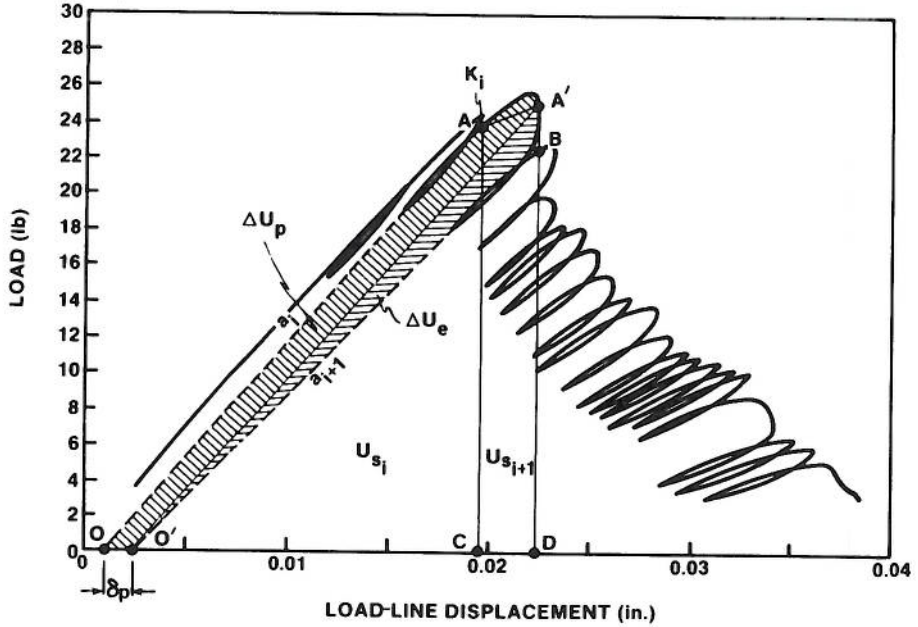

Figure 5. Partitioned load versus load-line displacement record for adhesive 3.

Figure 6 shows the width-normalized cumulative sums of the plastic energies dissipated and the elastic energies released as a function of the crack extension. As can be seen, G is the slope of the normalized cumulative released elastic energy and I is the slope of the normalized cumulative dissipated plastic energy. Also shown in Fig. 6 is the instantaneous value of the stored potential energy, U_s/B_n, at any crack extension. Neither of the curves is linear with respect to crack extension, i.e. their respective slopes are not constant and the values of G and I are not independent of the crack length.

Figure 7 illustrates this last feature with plots G and I versus crack extension. As shown, after an initial jump, both G and I decrease with crack extension. To ensure reliable correlations during the adhesive study in the presence of this crack-length dependence, we made all specimens identical in size and precracked them to the same initial crack length. All our comparisons of G and I were made at a crack growth of 0.030 in. (7.6 mm) beyond the initial crack length, since that interval generally coincides with the onset of stable crack growth. This point is indicated by the vertical dashed line in Fig. 7.

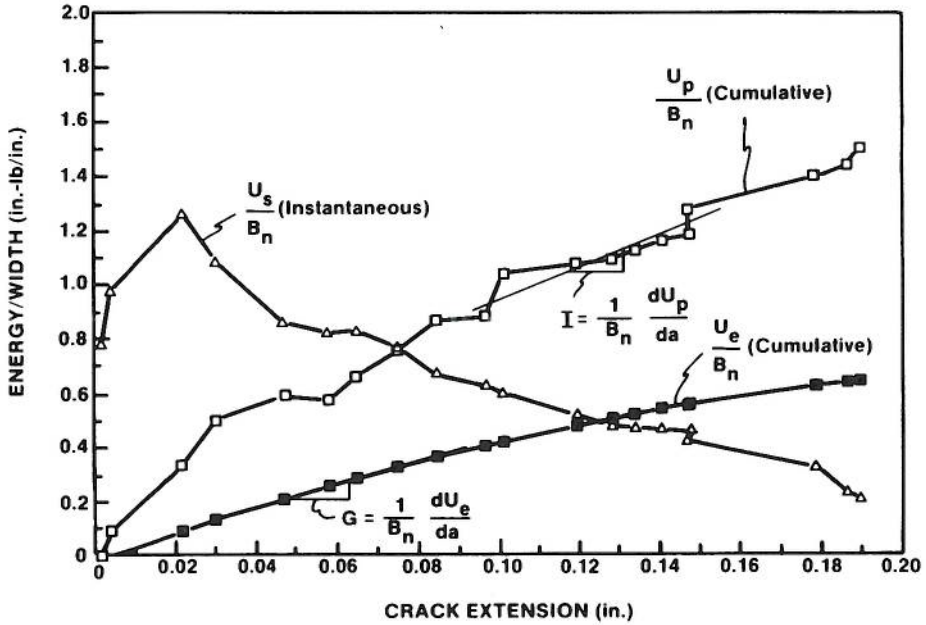

Figure 6. Cumulative energies released and stored versus crack extension for adhesive 3.

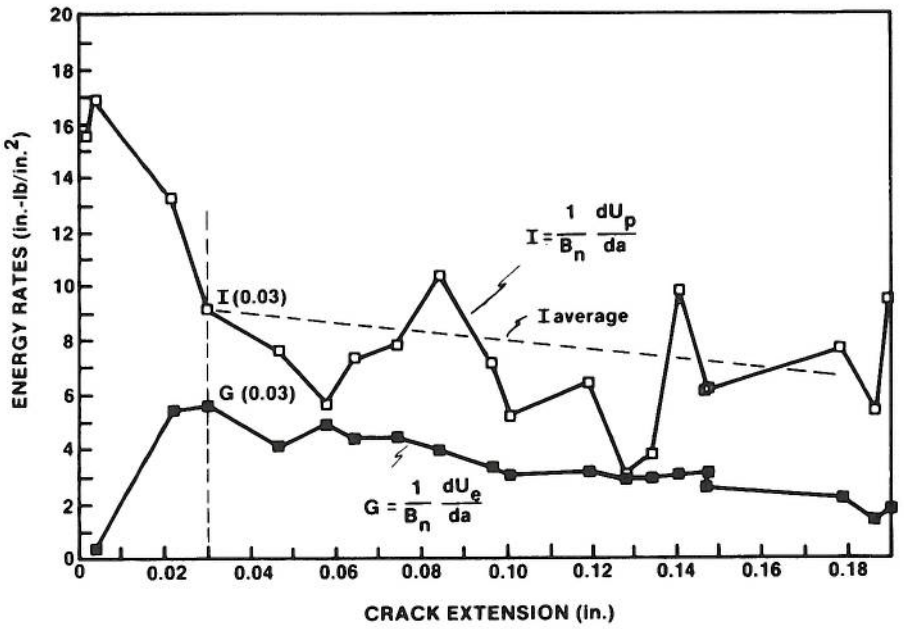

Figure 7. Elastic energy release rate and absolute plastic energy dissipation rate versus crack extension for adhesive 3.

3.3. Comparisons with the J integral

The validity of the energy separation technique can be assessed by comparing it with the J-integral method. In his original derivation of the J integral, Rice [6] was fairly explicit in relating J to body potential energy, whether the material behavior was linear or nonlinear. Rice *et al.* [7] assumed that elastic–plastic material behavior could be treated as non-linear elastic material behavior in the absence of unloading and concluded that J for the deeply cracked bend bar could be expressed as

$$J = 2A/B_n b, \tag{6}$$

where A is the total area under the load versus load-line displacement record, b is the remaining ligament of the test specimen, and B_n is the net width of the test specimen.

The coefficient of 'A' in equation (6) was modified to account for the tensile component of stress present in the compact tension specimen and was designated by 'η' [8].

In general, the current calculation of the J integral takes the form

$$J = \eta U/B_n b = J_{el} + J_{pl} = G_{es} + J_{pl} = \eta U_s/B_n b + \eta U_p/B_n b, \tag{7}$$

where J_{el} is the elastic component of J, J_{pl} is the plastic component of J, η is a coefficient related to the type of specimen, U is the total area under the load versus load-line displacement record, and U_s, U_p, B_n, b, and G_{es} are as defined previously.

For calculating the elastic energy release rate, G is now taken to be

$$G_q = K_q^2/E(1-\nu^2), \tag{8}$$

where K_q is the stress intensity factor as calculated from ASTM E399 [9].

We can now evaluate our technique against the J integral by comparing G calculated in several different ways with the values obtained from the energy separation method. It may be seen from equations (5), (7), and (8) that

$$G = K_q^2/E(1-\nu^2) = 1/B_n \, \mathrm{d}U_e/\mathrm{d}a = \eta U_s/B_n b, \tag{9}$$

which effectively relates the stress intensity factor, K_q, as calculated by ASTM E399, to the instantaneous potential energy of the test specimen, U_s, and also to the elastic energy released, U_e. Figure 8 illustrates the results of evaluating G by the three expressions: from K_q, as determined from ASTM E399; from energy separation using the increment of elastic energy released, $1/B_n(\mathrm{d}U_e/\mathrm{d}a)$; and from energy separation, but using the instantaneous value of the potential energy, $\eta U_s/B_n$, where $\eta = 2.3$. As can be seen, the results of all three calculations compare favorably in spite of plastic deformation, suggesting that the method of partitioning the different energies is consistent with current theory. The last calculation, i.e. $\eta U_s/B_n$, gives G at the initiation of unstable crack growth.

As a further benefit, the energy separation method allows more precise characterization of the plastic component of crack extension, a non-recoverable energy quantity. The J integral treats U_p (non-recoverable) as a component of the potential energy U_s (recoverable), whereas the energy separation method treats U_p as a post-crack extension quantity similar to U_e. As a consequence, the

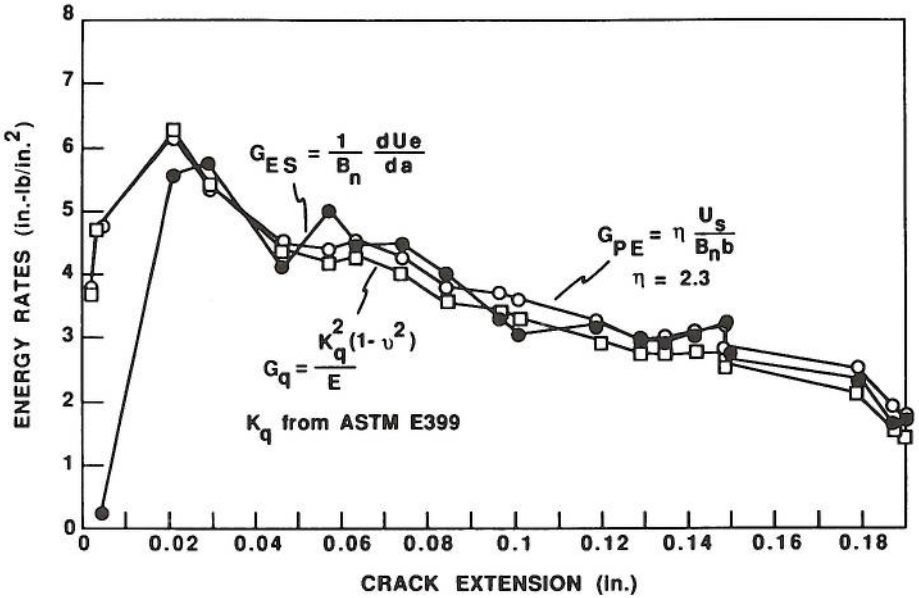

Figure 8. Elastic energy release rate, G, for neat adhesive 3 evaluated by three methods.

value of I becomes large, since U_p is divided by a small quantity, da, whereas J_{pl} becomes relatively small, since U_p is divided by the total remaining ligament b. Hence, the significance of U_p in the total quantity J might be lost. As we will show in our experimental results, G for our test adhesives does not vary dramatically, but the value of I can show substantial differences from one adhesive type to another.

4. RESULTS AND DISCUSSION

4.1. Stress relaxation

When a stress is applied to a viscous body, the body undergoes deformation so as to relieve the stress. The resulting decrease in stress with constant deformation is called stress relaxation. The deformation ceases when the stress level reaches a new equilibrium and the molecules or molecular segments return to their state of rest. At any time t, the stress, σ, in the deformed body is given by

$$\sigma = \sigma_0 \exp(t/t_{rel}), \tag{10}$$

where σ_0 is the initial stress and t_{rel} is the relaxation time, i.e. the time required for the stress to fall to $1/e$ of the original value.

At high RH, bulk adhesives absorb moisture and stress-relax under quasi-fixed displacements, in addition to the viscoelastic relaxation [4]. The stress-relaxation diagrams for adhesives 100 and 96 are shown in Fig. 4; Table 1 shows the results of relaxation testing on some of our adhesives. The locus of the high values represents the stress sustained by the adhesive immediately upon loading; the locus of the low values is the stress sustained after the adhesive reaches equilibrium with the 49°C (120°F), > 85% RH environment. Note that most of the adhesives lost a significant fraction of their 'dry' strength after loading in the

Table 1.
Stress-relaxation data

Sample	Equilibrium stress/initial stress (psi)			UTS (psi)
	2% strain	4% strain	6% strain	
1	500/2500	1600/2900	2300/3800	3600
12	100/1200	200/1400	300/1500	2800
13	700/2200	1200/3000	—	2500
100	20/200	40/200	60/500	3200
14[a]	900/2500	1700/3300	2000/3700	4800
15[a]	700/2500	1600/3700	2200/4100	10 000
17[a]	600/2500	1400/3200	1700/3900	6200
29[a]	800/2900	1500/3700	—	3700
30[a]	100/1500	300/1900	800/2400	5000
55[a]	1800/3700	2800/5000	3500/5500	6100
75[a]	500/1300	1000/2000	1500/2600	2700
85[a]	200/1200	500/1800	700/2100	1900
91[a]	1600/3400	2300/4700	2700/5300	5000
96[a]	1300/3000	2600/4200	3500/5500	7100

[a] Adhesives formulated in the program.

environment; adhesives 12, 30, and 100 retained only 10% or less of their initial values. However, quite a few adhesives retained 30% or more of their dry strength under testing. Given the severe nature of this test, these performances are considered quite satisfactory. Almost all the adhesives had good 'instantaneous' strengths (i.e. the stress values upon immediate loading at a given moisture–strain equilibrium), so that joints weakened by moisture would still have satisfactory properties under the type of transient stress likely to be experienced by structures such as an airframe or a mobile bridge.

4.2. Fracture analysis

4.2.1. Neat adhesives. Test results on the different neat adhesives showed wide variation in load magnitudes at crack initiation as well as in plastic deformation. Figures 9a–9c show typical unload compliance, load versus load-line displacement records for three neat adhesives: material that experienced a brittle, unstable failure at about 35 lb (77 kg) but was quite moisture-resistant; very tough but weakly adhesive material with little resistance to moisture; and a moderately tough and strong adhesive with some moisture resistance.

Some typical results for G and I are listed in Table 2 for fracture tests on our neat adhesive compact tension specimens; J is included for comparison and was calculated as defined by ASTM E1152 [5]. All values listed (average of three tests) were taken at a crack extension of 0.030 in. (7.6 mm). G and I were calculated by the energy separation method except in the case of brittle fracture, where G was calculated from equation (8). G within a single specimen was moderately constant over the crack extension examined; the standard deviation from specimen to specimen of the same type of adhesive was 20% or less. I values were more variable both within the same specimen and between specimens. Of all the variables influencing the tests results, crack extension was the most difficult to measure reliably. Crack-length measurements improved with

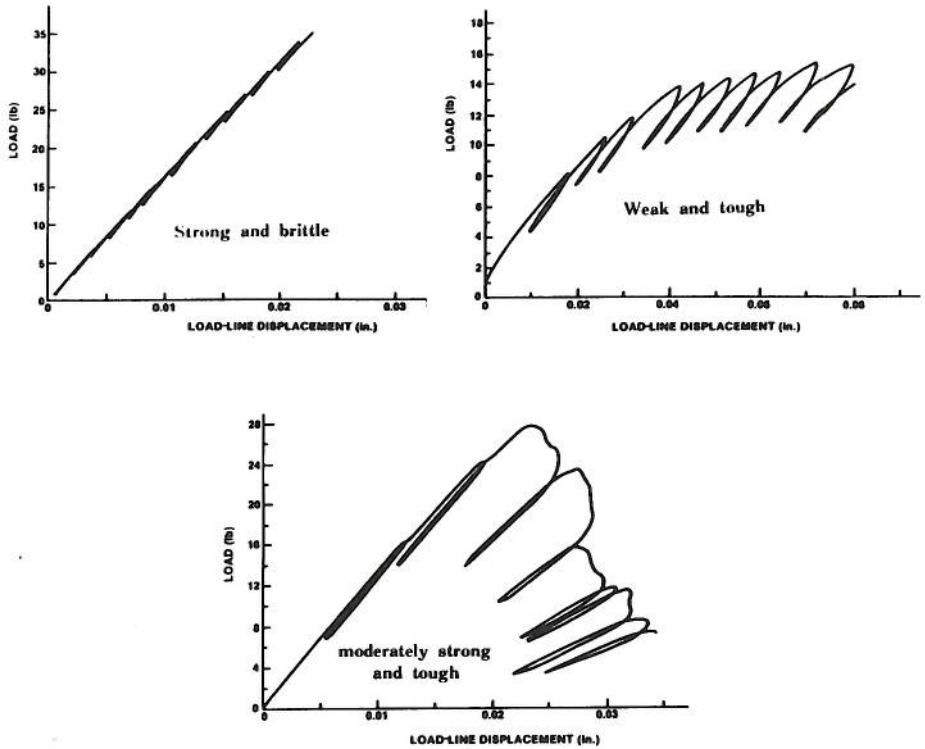

Figure 9. Load versus load-line displacement records for different adhesives.

Table 2.
Fracture toughness results on neat adhesive specimens

Adhesive	G (in.-lb/in.^{2})	G (J/m^2)	I (in.-lb/in.^{2})	I (J/m^2)	J (in.-lb/in.^{2})	J (J/m^2)	Peak load (lb)	Peak load (N)
1	3.7	(650)	4.2	(735)	4.7	(825)	32	(142)
3	8.3	(1450)	5.8	(1020)	10.9	(1910)	34	(151)
5	3.5	(615)	18.7	(3270)	8.8	(1540)	14	(62)
100	10.4	(1820)	27.7	(4850)	18.0	(3150)	58	(258)
14	11.0	(1930)	0		11.0[a]	(1930)	36	(160)
17	3.6	(630)	0		3.6[a]	(630)	28	(124)
96	7.2	(1260)	0		7.2[a]	(1260)	31	(138)
98	7.9	(1380)	0		7.9[a]	(1380)	35	(156)

[a] Specimen showed totally brittle behavior; $G = J$.

deeper unloadings, better determination of the values of E, and more accurate load-line displacement measurements.

The wide variations in I from adhesive to adhesive (Table 2) showed little or no correlation with elongation-to-failure data, as measured in a tensile test. Table 3 shows typical results of the neat specimen tensile testing. Of particular interest are adhesives 14 and 96, which showed moderate tensile elongations but completely brittle fracture, and adhesive 100, which showed low elongation but excellent fracture behavior.

Table 3.
Tensile test values for neat adhesives

Adhesive	Ultimate tensile strength (psi)	(MPa)	Modulus (ksi)	(MPa)	Elongation (%)
1	8960	(61.8)	410	(2830)	2.8
3	7650	(52.8)	330	(2280)	5.4
5	2160	(14.9)	110	(760)	10.6
100	8340	(57.5)	410	(2830)	2.8
14[a]	8830	(60.9)	330	(2280)	5.4
96[a]	10 710	(73.9)	390	(2690)	6.3
98[a]	9520	(61.8)	330	(2280)	4.9

[a]Denotes model adhesives developed for this program. The other adhesives are commercially available room-temperature-cure systems.

4.2.2. Bonded specimens. Fracture characterization data indicated that, in general, bonded specimens are more stable and tougher than the neat specimens. Figure 10 shows load versus load-line displacement plots of a 1/2T CT plan neat specimen and a bonded test specimen identical in size and type for the same adhesive. As can be seen, the stiffer bonded specimen exhibits considerably less load-line displacement than the neat specimen, and withstands over three times the load; the bulk specimen in this case is completely brittle. Typical results for bonded specimens are presented in Table 4.

The value of G for bonded specimens was similar to, but slightly lower than, that for the neat specimens, and bondline failure was nearly always cohesive in these cases. When the bondline failed at the adhesive–adherend interface, the

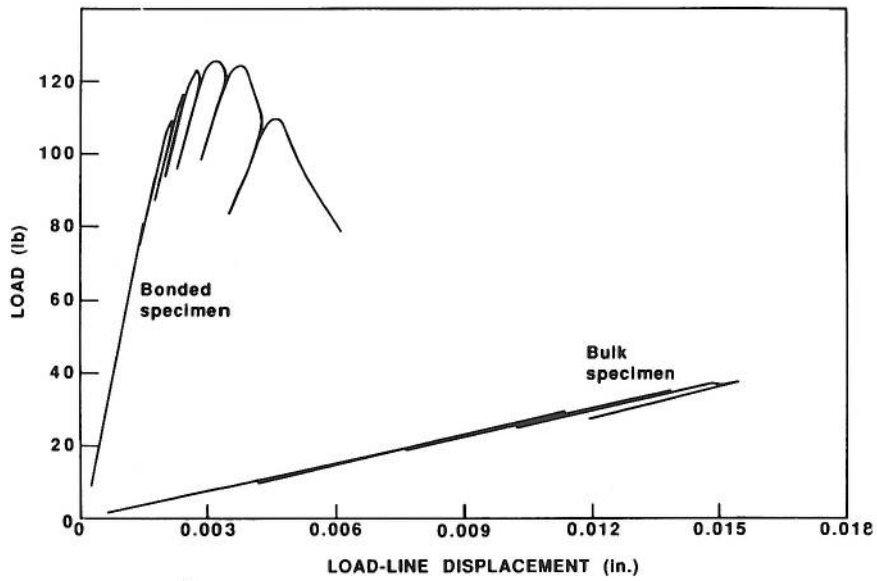

Figure 10. Comparison of the load versus load-line displacement records for bonded and neat specimens of adhesive 14.

Table 4.
Fracture toughness test results for bonded specimens

Adhesive	G (in.-lb/in.^{2})	G (J/m^2)	I (in.-lb/in.^{2})	I (J/m^2)	J (in.-lb/in.^{2})	J (J/m^2)	Peak load (lb)	Peak load (N)
1	4.2	(735)	10.7	(3470)	4.5	(790)	149	(663)
3	4.9	(860)	12.4	(2170)	7.1	(1240)	138	(614)
5	3.5	(610)	11.9	(2080)	3.0	(525)	75	(334)
100	8.2	(1450)	40.0	(7000)	11.0	(1930)	214	(952)
14	3.8	(665)	1.2	(210)	2.1	(370)	131	(583)
96	4.0	(700)	2.7	(470)	4.1	(719)	111	(494)
98	7.9	(1380)	0		7.9[a]	(1380)	111	(494)

[a] Specimen showed totally brittle behavior; $G = J$.

value of G dropped substantially. I for the bonded specimens was routinely higher, consistent with their more stable crack growth.

4.2.3. Stiffness considerations. The most probable explanation for the differences in behavior observed is the substantial disparity in stiffness for the two types of specimens. The aluminum adherends, which are quite stiff relative to the bondline adhesive, allow a more uniform rotation of the specimen during loading and, thus, a more uniform distribution of stress over the entire bondline. As a result, the concentration of stress at the crack tip is reduced, allowing the specimen to sustain a higher load. On the other hand, the more flexible neat specimen, as demonstrated by its greater load-line displacement, tends to 'peel' apart, concentrating stresses nearer the crack tip; thus, a smaller load can initiate crack growth. Greater material stiffness would thus appear to be beneficial to a bonded joint since it confers the distinct advantage of higher load capacity without loss of fracture resistance.

5. CONCLUSIONS

We have observed to date that the ductility of structural adhesives decreases as moisture resistance increases, and thus any adhesive modification program must concurrently monitor the changes in both properties. This can be readily accomplished by a combination of stress-relaxation measurements on thin strips of adhesive and unload compliance analysis on 1/2T compact tension specimens of both neat and bonded adhesives.

For the stress-relaxation measurements, the locus of the lowest points of all segments represents the equilibrium tensile stress–strain curve, i.e. the strain at which the moisture content in the adhesive is in equilibrium with the RH of the environment. The adhesive stress-relaxes under fixed displacement mostly due to swelling/water reorganization mechanisms during moisture absorption. A third mechanism involving the breakage of crosslinks becomes pronounced as the 'yield' point of the adhesive is approached. Most of the adhesives we tested lost a significant fraction (more than 90%) of their dry strength after loading in a 49°C (120°F) and $> 85\%$ RH environment. In view of the nature of the test and the susceptibility of epoxy adhesives to moisture-induced degradation, adhesives retaining more than 30% of their dry strength under these conditions are considered satisfactory.

The energy separation method described here allows G to be measured directly from the test record using either the increment of released energy, dU_e, or the instantaneous value of the potential energy, U_s. Either measurement correlates well with current theory. The parameter I, as derived with the energy separation method, provides a distinct and sensitive measure of the plastic component of fracture resistance. Compared with neat adhesive specimens, bonded specimens sustain more than three times the load at crack initiation, and consistently exhibit greater crack-growth stability, even when the neat specimens show brittle behavior.

Due to the under-representation of the plastic energy component, I, in the computation of the fracture parameter, J, these calculated values suggest that the neat adhesive specimens resist crack growth better than the bonded specimens, contrary to experimental observation. Results of the energy separation technique, however, clearly show the superiority of the bonded specimens in resisting crack growth, as reflected in the values of I.

Since all of the fracture parameters discussed in this study are dependent on the crack length, care must be taken to maintain consistent specimen size and geometry, including the initial crack length.

Acknowledgement

We gratefully acknowledge financial support for this work from the U.S. Army Troop Support Command's Belvoir Research, Development, and Engineering Center under Contract No. DAAK70-86-C-0084.

REFERENCES

1. C. O. Arah, J. Vogin, D. McNamara, J. Ahearn, A. Berrier and G. Davis, in: *Proc. 5th Joint Government–Industry Symp. on Structural Adhesive Bonding*, pp. 440–458. Picatinny Arsenal, ADPA, Washington, DC (1987).
2. M. F. Mecklenburg, J. Joyce and P. Albrecht, *Am. Soc. Test. Mater., Spec. Tech. Publ.* **995** (in press).
3. J. A. Joyce and J. Gudas, *Am. Soc. Test. Mater., Spec. Tech. Publ.* **668**, 451–468 (1979).
4. P. Albrecht, M. F. Mecklenburg, J. Wang and W. Hong, *Effect of Environment on Mechanical Properties of Adhesives*, Final Report, Office of Research, Development, and Technology, Federal Highway Administration, Contract No. DTFH-61-84C-00027 (February 1987).
5. *ASTM E1152-87*, American Society for Testing and Materials, Philadelphia, PA (1987).
6. J. R. Rice, *J. Appl. Mech.* **35**, 379 (1968).
7. J. R. Rice, P. C. Paris and J. G. Merkle, *Am. Soc. Test. Mater., Spec. Tech. Publ.* **536**, 231–245 (1973).
8. C. E. Turner, *Am. Soc. Test. Mater., Spec. Tech. Publ.* **700**, 314.
9. *ASTM E399-83*. American Society for Testing and Materials, Philadelphia, PA (1983).